

# Characterization of timing jitter in a 5 GHz quantum dot passively mode-locked laser

Chang-Yi Lin,<sup>1,\*</sup> Frederic Grillot,<sup>2</sup> Yan Li,<sup>1</sup> Ravi Raghunathan,<sup>1</sup> and Luke F. Lester<sup>1</sup>

<sup>1</sup>Center for High Technology Materials, University of New Mexico, 1313 Goddard SE, Albuquerque, NM 87106, USA

<sup>2</sup>Université Européenne de Bretagne, INSA, CNRS- Laboratoire FOTON, 20 avenue des buttes de Coesmes, 35708 Rennes, Cedex 7, France

\*[cylin@unm.edu](mailto:cylin@unm.edu)

**Abstract:** The timing jitter performance of a 5 GHz quantum dot passively mode-locked laser is investigated at different harmonics in the RF spectrum. The necessity of measuring the phase noise at relatively large harmonic numbers is motivated experimentally in the context of determining the corner frequency, its correlation to the RF linewidth, and the related white noise plateau level. The single-sideband phase noise with an integrated timing jitter of 211 fs (4-80 MHz) is reported. An all-microwave technique has been used to determine a pulse-to-pulse rms timing jitter of 96 fs/cycle. This low timing jitter value makes the chip-scale quantum dot mode-locked laser an attractive source for low noise applications such as optical clocking and sampling.

©2010 Optical Society of America

**OCIS codes:** (140.4050) Mode-locked lasers; (140.5960) Semiconductor lasers; (250.5590) Quantum-well, -wire and -dot devices

---

## References and links

1. G. Carpintero, M. G. Thompson, R. V. Penty, and I. H. White, "Low noise performance of passively mode-locked 10-GHz quantum dot laser diode," *IEEE Photon. Technol. Lett.* **21**(6), 389–391 (2009).
2. A. Akrou, A. Shen, A. Enard, G.-H. Duan, F. Lelarge, and A. Ramdane, "Low phase noise all-optical oscillator using quantum dash modelocked laser," *Electron. Lett.* **46**(1), 73–73 (2010).
3. S. Breuer, W. Elsaer, J. G. McInerney, K. Yvind, J. Pozo, E. A. J. M. Bente, M. Yousefi, A. Villafranca, N. Vogiatzis, and J. Rorison, "Investigations of Repetition Rate Stability of a Mode-Locked Quantum Dot Semiconductor Laser in an Auxiliary Optical Fiber Cavity," *IEEE J. Quantum Electron.* **46**(2), 150–157 (2010).
4. M. G. Thompson, D. Larsson, A. Rae, K. Yvind, R. V. Penty, I. H. White, J. Hvam, A. R. Kovsh, S. Mikhrin, D. Livshits, and I. Krestnikov, "Monolithic hybrid and passive mode-locked 40 GHz quantum dot laser diodes," *Proc. Eur. Conf. Opt. Commun. (ECOC)*, 1–2 (2006).
5. E. U. Rafailov, M. A. Cataluna, and W. Sibbett, "Mode-locked quantum-dot lasers," *Nat. Photonics* **1**(7), 395–401 (2007).
6. M. G. Thompson, A. R. Rae, M. Xia, R. V. Penty, and I. H. White, "InGaAs quantum-dot mode-locked laser diodes," *IEEE J. Sel. Top. Quantum Electron.* **15**, 661–672 (2009).
7. Y.-C. Xin, Y. Li, A. Martinez, T. J. Rotter, H. Su, L. Zhang, A. L. Gray, S. Luong, K. Sun, Z. Zou, J. Zilko, P. M. Varangis, and L. F. Lester, "Optical gain and absorption of quantum dots measured using an alternative segmented contact method," *IEEE J. Quantum Electron.* **42**(7), 725–732 (2006).
8. L. Zhang, L.-S. Cheng, A. L. Gray, H. Huang, S. Kuty, H. Li, J. Nagyvary, F. Nabulsi, L. Olona, E. Pease, Q. Sun, C. Wiggins, J. C. Zilko, Z. Zou, and P. M. Varangis, "High-power low-jitter quantum-dot passively mode-locked lasers," *Proc. SPIE* **6115**, 611502 (2006).
9. D. Von der Linde, "Characterization of noise in continuously operating mode-locked lasers," *Appl. Phys., B Photophys. Laser Chem.* **39**(4), 201–217 (1986).
10. J. P. Tourrenc, A. Akrou, K. Merghem, A. Martinez, F. Lelarge, A. Shen, G. H. Duan, and A. Ramdane, "Experimental investigation of the timing jitter in self-pulsating quantum-dash lasers operating at 1.55  $\mu\text{m}$ ," *Opt. Express* **16**(22), 17706–17713 (2008).
11. D. Eliyahu, R. A. Salvatore, and A. Yariv, "Noise characterization of pulse train generated by actively mode-locked lasers," *J. Opt. Soc. Am. B* **13**(7), 1619–1626 (1996).
12. "The control of jitter and wander within the optical transport network," Recommendation G.8251, ITU-T, (2001).
13. D. Eliyahu, R. A. Salvatore, and A. Yariv, "Effect of noise on the power spectrum of passively mode-locked lasers," *J. Opt. Soc. Am. B* **14**(1), 167–174 (1997).
14. F. Kefelian, S. O'Donoghue, M. T. Todaro, J. G. McInerney, and G. Huyet, "RF linewidth in monolithic passively mode-locked semiconductor laser," *IEEE Photon. Technol. Lett.* **20**(16), 1405–1407 (2008).

15. T. Yilmaz, C. M. Depriest, A. Braun, J. H. Abeles, and P. J. Delfyett, "Noise in Fundamental and Harmonic Modelocked Semiconductor Lasers: Experiments and Simulations," *IEEE J. Quantum Electron.* **39**(7), 838–849 (2003).
  16. C.-Y. Lin, F. Grillot, N. A. Naderi, Y. Li, and L. F. Lester, "rf linewidth reduction in a quantum dot passively mode-locked laser subject to external optical feedback," *Appl. Phys. Lett.* **96**(5), 051118 (2010).
  17. C.-Y. Lin, F. Grillot, Y. Li, R. Raghunathan, and L. F. Lester, "Characterization of timing jitter in a quantum dot passively mode-locked laser at low offset frequency," submitted to IEEE Photonics Society Annual Conference (2010).
  18. Y.-C. Xin, Y. Li, V. Kovanis, A. L. Gray, L. Zhang, and L. F. Lester, "Reconfigurable quantum dot monolithic multisection passive mode-locked lasers," *Opt. Express* **15**(12), 7623–7633 (2007).
- 

## 1. Introduction

Effective and compact semiconductor passively mode-locked lasers (MLLs) have been attracted plenty of attention due to the demand of ultra-low phase noise optoelectronic oscillators for optical signal processing applications [1–4]. These applications include high speed optical sampling, all-optical clock recovery and clock distribution. Quantum dot (QD) materials offer several potential advantages to improve the timing jitter performance of a passive MLL, such as reduced internal loss, low spontaneous emission noise, and low linewidth enhancement factor [5,6]. However, in contrast to active mode-locking, the timing stability issue (nonstationary processes) is the main disadvantage of passive MLLs due to the lack of an external reference source. Since timing fluctuations in the optical pulse train play an important role in determining the laser performance, it is crucial that the jitter characterization in a passive MLL be studied more thoroughly.

In this paper, we experimentally characterize the corner frequency and low-frequency plateau level in the phase noise of a nonstationary monolithic two-section passive QD MLL operating with a nominal 5 GHz repetition rate. The device exhibits a state-of-art integrated timing jitter value of 211 fs (4–80 MHz) and a pulse-to-pulse root mean square (rms) timing jitter of 96 fs/cycle for a 5 GHz passive QD MLL.

## 2. Device structure and fabrication

The QD structure investigated in this work was grown by elemental source molecular beam epitaxy on an  $n^+$ -doped (100) GaAs substrate. The active region consists of six "Dots-in-a-Well" (DWELL) layers. In each layer, an equivalent coverage of 2.4 monolayer InAs QDs is confined approximately in the middle of a 10 nm  $\text{In}_{0.15}\text{Ga}_{0.85}\text{As}$  quantum well (QW) [7]. The epitaxial structure and waveguide design are displayed in Fig. 1(a). The 3- $\mu\text{m}$ -wide ridge-waveguide devices were etched by inductively coupled plasma (ICP) etching and planarized using benzocyclobutene (BCB). Ti/Pt/Au was then deposited to form the p-metal contact. The electrical isolation between the gain and absorber sections was provided by proton implantation with an isolation resistance of  $>10\text{ M}\Omega$ . After the substrate had been thinned and polished, a Ge/Au/Ni/Au n-metal contact was deposited on the backside of the  $n^+$ -GaAs substrate and annealed at  $\sim 380^\circ\text{C}$  for 1 minute to form the n-ohmic contact. The two-section QD passive MLLs were made with a total cavity length of 7.8-mm and a saturable absorber (SA) length of 1.1-mm. The nominal repetition rate of the QD MLL is 5 GHz. A highly reflective coating ( $R \approx 95\%$ ) was applied to the mirror facet next to the SA to create self-colliding pulse effects in the SA for pulse narrowing, and the output facet was cleaved ( $R \approx 32\%$ ). The devices were p-side-up mounted on AlN heatsink carriers. These chip-on-carriers were then packaged into an industry-standard 14-pin butterfly packages with a thermoelectric cooler (TEC) and a polarization-maintaining lensed fiber pigtail as shown in Fig. 1(b) [8]. The function of the packaged module is to reduce environmental noise and enhance mechanical stability. The fiber-coupled light-current (L-I) curve under  $-7\text{ V}$  reverse voltage bias condition at  $20^\circ\text{C}$  is displayed in Fig. 2. The inset is the optical spectrum showing the peak lasing wavelength at 1.33- $\mu\text{m}$  under a gain current of 90 mA and an SA reverse voltage of  $-7\text{ V}$ . The typical average powers emitted by these devices under mode-locking conditions at the end of the fiber pigtail are 1–2.5 mW. The pulse durations are on the order of 10 ps. The time-bandwidth product of the MLL typically ranges from 2 to 10.

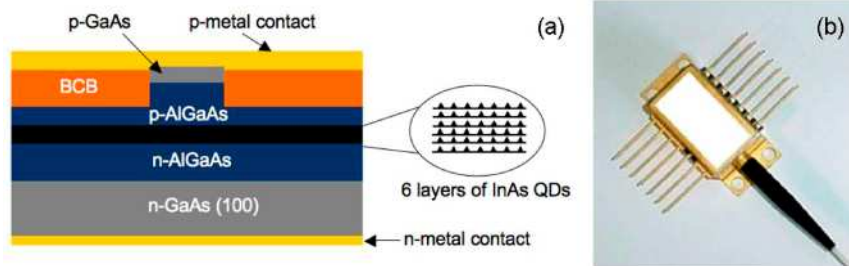


Fig. 1. (a) Schematic of the epitaxial layer structure of the InAs QD laser. (b) Picture of the passive QD MLL packaged module.

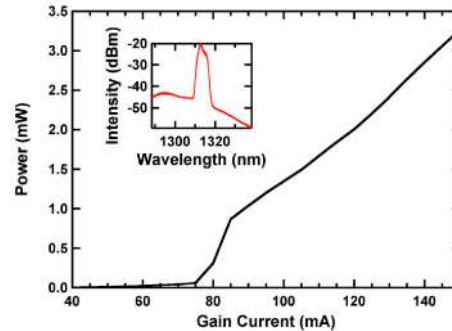


Fig. 2. L-I characteristic measured at 20°C for an absorber bias of -7 V. The inset shows the optical spectrum under 90 mA gain current and -7 V reverse voltage.

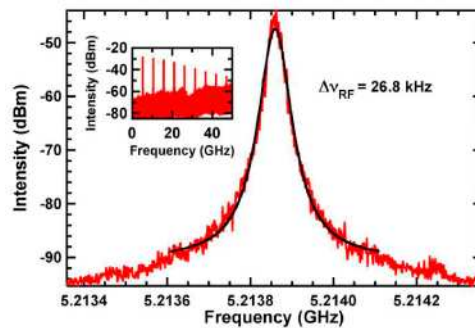


Fig. 3. RF linewidth of 26.8 kHz under 90 mA gain current and -7 V reverse voltage. The inset shows the full span RF spectrum at the same bias condition.

### 3. Characterization results and discussion

The rms timing jitter characterization is performed via a 45 GHz bandwidth photodiode coupled to an Agilent 8565EC electrical spectrum analyzer (ESA) that has a 50 GHz frequency range. Since above the corner frequency, the phase noise in our QD MLL scales with harmonic number, the rms timing jitter is calculated by integrating the single-sideband phase noise (SSB-PN) spectral density,  $L(f)$ , using the following expression [9]:

$$\sigma = \frac{1}{2\pi n f_R} \sqrt{2 \int_{f_{\min}}^{f_{\max}} L(f) df} \quad (1)$$

where  $n$  is the number of the harmonic at which the phase noise is measured,  $f_R$  is the repetition frequency, and  $f_{\min}$  and  $f_{\max}$  determine the offset frequency range over which the  $L(f)$  is integrated. In contrast to previous optical cross-correlation techniques [10], microwave data on the corner frequency and white noise plateau level across the 8 harmonics tested is used to calculate the pulse-to-pulse rms timing jitter [11].

The optimum 3-dB RF linewidth shown in Fig. 3 is 26.8 kHz under a 90 mA DC bias on the gain section and  $-7$  V applied to the absorber. The inset shows the full-span RF spectrum at the same bias condition. The RF linewidth is confirmed with a Lorentzian curve fitting through the ESA with a resolution bandwidth of 1 kHz. Figure 4(a) displays the SSB-PN spectra,  $L(f)$ , for different harmonics of the 5 GHz passive MLL device. The relatively low repetition rate of this monolithic passive MLL makes the characterization of higher order harmonics possible and all harmonics are phase noise dominated as confirmed in Fig. 4(b). Above the corner frequency, the phase noise trace shows the typical roll-off with a slope of  $-20$  dBc/Hz per decade until it hits the thermal noise floor. For communication system applications, the MLL is to be used as a transmitter, where clock-recovery is performed in the receiver. Consequently, the jitter on a very long timescale will not matter, as this will be trivially tracked by the clock-recovery circuit. Integration of the SSB-PN using the ITU-T specified range gives a timing jitter of 390 fs at the 3rd harmonic order (4 MHz to 80 MHz) as shown in Fig. 4(c) [12]. The phase noise trace hits the thermal noise floor at the offset frequency of 9 MHz. Thus, extrapolating the trace from 9 MHz at the standard roll-off of  $-20$  dBc/Hz per decade results in a timing jitter value of 211 fs, the lowest reported to date of a 5 GHz passive MLL. From the data presented in Fig. 4(a), the pulse-to-pulse rms timing jitter,  $\sigma_{pp}$ , can be calculated using the nonstationary passive MLL theory of Eq. (23) in [11]. The associated curve-fits to the 8 harmonics give an average  $\sigma_{pp}$  of  $96 \pm 10$  fs/cycle.

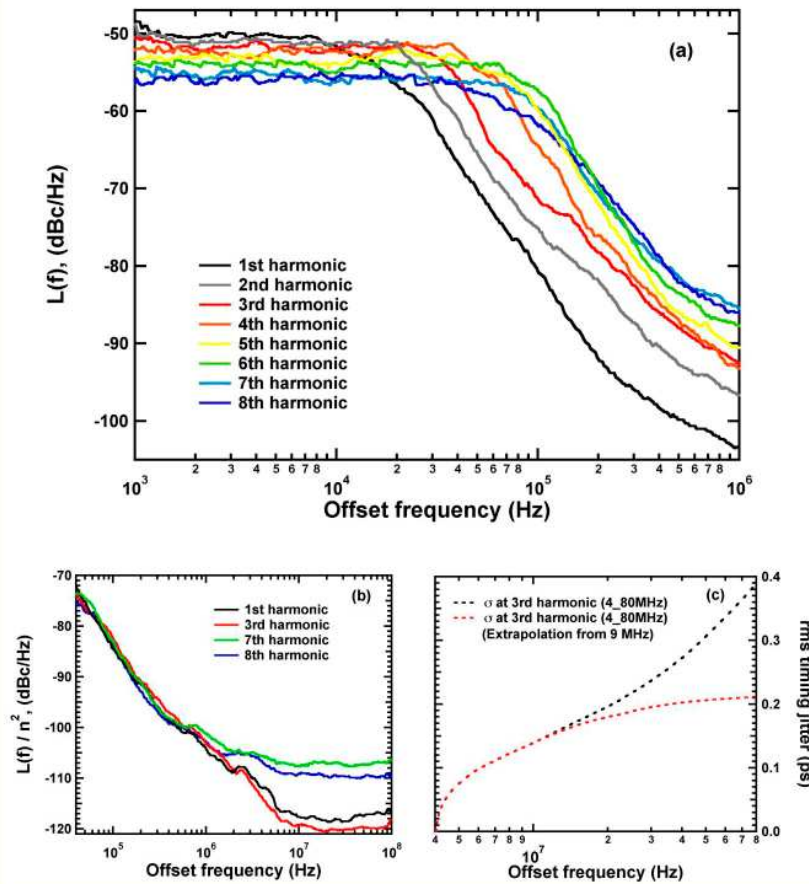


Fig. 4. (a) SSB-PN spectra density from different harmonics under 90 mA gain current and  $-7$  V reverse voltage. (b) SSB-PN spectra density above the corner frequency normalized to  $n^2$  from different harmonics under the same bias condition as (a). (c) Timing jitter at the 3rd harmonic over the offset frequency range of 4 MHz to 80 MHz.

Further noise performance of the passive MLL is investigated at different bias conditions. Figure 5(a) and (b) demonstrate the RF linewidth under  $-7$  V applied to the absorber and 110 mA and 130 mA DC bias on the gain section, respectively. As seen in these figures, the RF linewidth broadens with increasing gain current to 95.4 (110 mA) and 294 kHz (130 mA), which implies that the pulse-to-pulse rms timing jitter should also rise [13,14]. The SSB-PN spectra at the 3rd harmonic under different bias currents and  $-7$  V reverse voltage are shown in Fig. 6. It clearly demonstrates that the corner frequency increases from 14 kHz to 200 kHz to 1.6 MHz, as the gain current is raised from 90 mA to 110 mA and then 130 mA DC bias, respectively. Concurrently, the white-noise plateau does decrease since the total power of the oscillator has not changed much but the phase noise has broadened the spectral linewidth significantly. Thus, the corner frequency is a good figure-of-merit for MLLs regarding pulse timing stability. Here, it is empirically found from the data that the corner frequency varies as the square of the RF linewidth.

In contrast to actively mode-locked lasers [15], the pulse train timing stability issue is still the main disadvantage of passive MLLs due to the lack of an external reference source. However, several methods have been proposed to reduce the phase noise in passive MLLs such as injection locking or external optical feedback [2,3,16]. Under the resonant feedback condition, the RF linewidth can be reduced which results in a smaller jitter value than the free-running case. The feedback effect has also been observed to improve the corner frequency down to a lower offset frequency level [17]. The detailed investigation of the external feedback effect on SSB-PN spectra will be discussed in a future paper. Furthermore, hybrid mode-locking techniques can also be used for lowering the white-noise plateau level of a MLL [1].

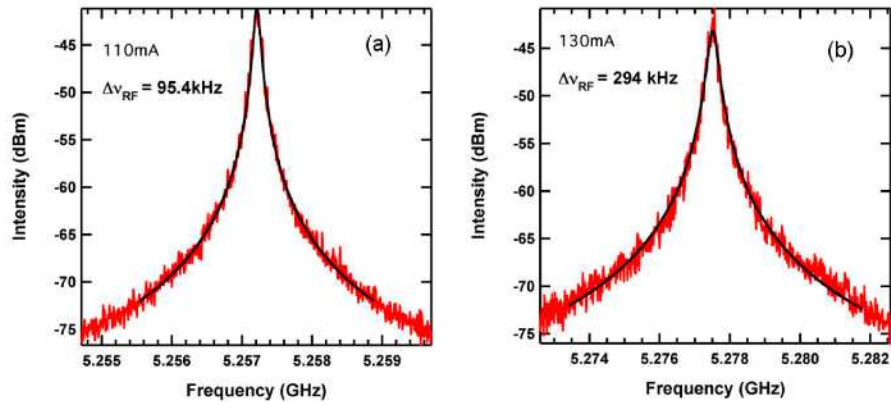


Fig. 5. (a) RF linewidth of 95.4 kHz under 110 mA gain current and  $-7$  V reverse voltage. (b) RF linewidth of 294 kHz under 130 mA gain current and  $-7$  V reverse voltage. The black curves represent the Lorentzian curve-fitting results.

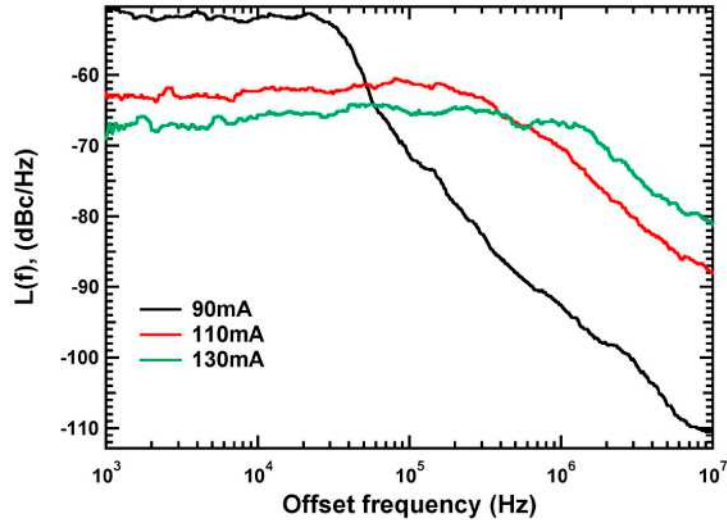


Fig. 6. SSB-PN spectra density at the 3rd harmonic under 90, 110, and 130 mA gain current and  $-7$  V reverse voltage.

#### 4. Conclusion

To the best of our knowledge, this is the first time that the relationships between the timing jitter, RF linewidth, and SSB-PN corner frequency and white-noise plateau in a monolithic passive QD MLL have been discussed. A state-of-the-art timing jitter value of 211 fs (4 MHz to 80 MHz) for a 5 GHz passive QD MLL has been reported. The best jitter and lowest corner frequency was found just above the threshold current of the MLL and then typically the performance degraded with increasing current bias in the gain section at a fixed absorber voltage. In general this behavior mirrors the trend in the pulse quality, which has been reported previously [18]. The wide offset frequency span examined (1 kHz to 100MHz) gives a better understanding of the noise performance at and below the corner frequency, which provides an alternative all-microwave method to obtain the pulse-to-pulse rms timing jitter. Further improvement of noise performance and corner frequency could be achieved under injection locking or external optical feedback.

#### Acknowledgments

This work was supported by the Air Force Office of Scientific Research under Grant Nos. FA9550-06-1-0411 and FA9550-09-1-0490.